Research Article | Vol. 7, No. 11 | 1 Nov 2016 | BIOMEDICAL OPTICS EXPRESS 4803
Biomedical Optics EXPRESS

Simple approach to three-color two-photon microscopy by a fiber-optic wavelength convertor

KUEN-CHE LI,[1,5] LYNN L. H. HUANG,[2,3,4,5] JHIH-HAO LIANG,[3] AND MING-CHE CHAN[1,*]

[1]College of Photonics, National Chiao-Tung University, Taiwan
[2]Department of Biotechnology and Bioindustry Sciences, National Cheng Kung University, Taiwan
[3]Institute of Biotechnology, National Cheng Kung University, Taiwan
[4]Research Center of Excellence in Regenerative Medicine, National Cheng Kung University, Taiwan
[5]Equal contribution
[*]mcchan@nctu.edu.tw

Abstract: A simple approach to multi-color two-photon microscopy of the red, green, and blue fluorescent indicators was reported based on an ultra-compact 1.03-μm femtosecond laser and a nonlinear fiber. Inside the nonlinear fiber, the 1.03-μm laser pulses were simultaneously blue-shifted to 0.6~0.8 μm and red-shifted to 1.2~1.4 μm region by the Cherenkov radiation and fiber Raman gain effects. The wavelength-shifted 0.6~0.8 μm and 1.2~1.4 μm radiations were co-propagated with the residual non-converted 1.03-μm pulses inside the same nonlinear fiber to form a fiber-output three-color femtosecond source. The application of the multi-wavelength sources on multi-color two-photon fluorescence microscopy were also demonstrated. Overall, due to simple system configuration, convenient wavelength conversion, easy wavelength tunability within the entire 0.7~1.35 μm bio-penetration window and less requirement for high power and bulky light sources, the simple approach to multi-color two-photon microscopy could be widely applicable as an easily implemented and excellent research tool for future biomedical and possibly even clinical applications.

OCIS codes: (110.4234) Multispectral and hyperspectral imaging; (180.2520) Fluorescence microscopy; (180.4315) Nonlinear microscopy; (060.4370) Nonlinear optics, fibers; (320.7110) Ultrafast nonlinear optics.

References and links

1. W. Denk, J. H. Strickler, and W. W. Webb, "Two-photon laser scanning fluorescence microscopy," Science **248**(4951), 73–76 (1990).
2. K. König, "Multiphoton microscopy in life sciences," J. Microsc. **200**(2), 83–104 (2000).
3. P. N. Prasad, *Introduction to Biophotonics* (John Wiley & Sons Inc., New Jersey, 2003).
4. J. M. Squirrell, D. L. Wokosin, J. G. White, and B. D. Bavister, "Long-term two-photon fluorescence imaging of mammalian embryos without compromising viability," Nat. Biotechnol. **17**(8), 763–767 (1999).
5. I.-H. Chen, S.-W. Chu, C.-K. Sun, P. C. Cheng, and B.-L. Lin, "Wavelength dependent cell damages in multi-photon confocal microscopy: A micro-spectroscopic comparison between femtosecond Ti:sapphire and Cr:forsterite laser sources," Opt. Quantum Electron. **34**(12), 1251–1266 (2002).
6. D. Kobat, M. E. Durst, N. Nishimura, A. W. Wong, C. B. Schaffer, and C. Xu, "Deep tissue multiphoton microscopy using longer wavelength excitation," Opt. Express **17**(16), 13354–13364 (2009).
7. M. E. Dickinson, E. Simbuerger, B. Zimmermann, C. W. Waters, and S. E. Fraser, "Multiphoton excitation spectra in biological samples," J. Biomed. Opt. **8**(3), 329–338 (2003).
8. M. C. Chan, T. M. Liu, S. P. Tai, and C.-K. Sun, "Compact fiber-delivered Cr:Forsterite laser for nonlinear light microscopy," J. Biomed. Opt. **10**(5), 054006 (2005).
9. S. Sakadzić, U. Demirbas, T. R. Mempel, A. Moore, S. Ruvinskaya, D. A. Boas, A. Sennaroglu, F. X. Kaertner, and J. G. Fujimoto, "Multi-photon microscopy with a low-cost and highly efficient Cr:LiCAF laser," Opt. Express **16**(25), 20848–20863 (2008).
10. D. Isailovic, Y. Xu, T. Copus, S. Saraswat, and S. M. Nauli, "Multimodal Spectral Imaging of Cells Using a Transmission Diffraction Grating on a Light Microscope," Appl. Spectrosc. **65**(6), 575–583 (2011).
11. X. Gao, Y. Cui, R. M. Levenson, L. W. K. Chung, and S. Nie, "In vivo cancer targeting and imaging with semiconductor quantum dots," Nat. Biotechnol. **22**(8), 969–976 (2004).

#274506 http://dx.doi.org/10.1364/BOE.7.004803
Journal © 2016 Received 25 Aug 2016; revised 13 Oct 2016; accepted 25 Oct 2016; published 31 Oct 2016

Biomedical Optics EXPRESS

12. V. N. Belov, M. L. Bossi, J. Fölling, V. P. Boyarskiy, and S. W. Hell, "Rhodamine Spiroamides for Multicolor Single-Molecule Switching Fluorescent Nanoscopy," Chemistry **15**(41), 10762–10776 (2009).
13. F. Humpert, I. Yahiatène, M. Lummer, M. Sauer, and T. Huser, "Quantifying molecular colocalization in live cell fluorescence microscopy," J. Biophotonics **8**(1-2), 124–132 (2015).
14. J. Livet, T. A. Weissman, H. Kang, R. W. Draft, J. Lu, R. A. Bennis, J. R. Sanes, and J. W. Lichtman, "Transgenic strategies for combinatorial expression of fluorescent proteins in the nervous system," Nature **450**(7166), 56–62 (2007).
15. Z. Fan, J. A. Spencer, Y. Lu, C. M. Pitsillides, G. Singh, P. Kim, S. H. Yun, V. Toxavidis, T. B. Strom, C. P. Lin, and M. Koulmanda, "In vivo tracking of 'color-coded' effector, natural and induced regulatory T cells in the allograft response," Nat. Med. **16**(6), 718–722 (2010).
16. K. Weber, M. Thomaschewski, M. Warlich, T. Volz, K. Cornils, B. Niebuhr, M. Täger, M. Lütgehetmann, J. M. Pollok, C. Stocking, M. Dandri, D. Benten, and B. Fehse, "RGB marking facilitates multicolor clonal cell tracking," Nat. Med. **17**(4), 504–509 (2011).
17. K. Hope and M. Bhatia, "Clonal interrogation of stem cells," Nat. Methods **8**(4 Suppl), S36–S40 (2011).
18. D. Entenberg, J. Wyckoff, B. Gligorijevic, E. T. Roussos, V. V. Verkhusha, J. W. Pollard, and J. Condeelis, "Setup and use of a two-laser multiphoton microscope for multichannel intravital fluorescence imaging," Nat. Protoc. **6**(10), 1500–1520 (2011).
19. P. Mahou, M. Zimmerley, K. Loulier, K. S. Matho, G. Labroille, X. Morin, W. Supatto, J. Livet, D. Débarre, and E. Beaurepaire, "Multicolor two-photon tissue imaging by wavelength mixing," Nat. Methods **9**(8), 815–818 (2012).
20. K. Wang, T.-M. Liu, J. Wu, N. G. Horton, C. P. Lin, and C. Xu, "Three-color femtosecond source for simultaneous excitation of three fluorescent proteins in two-photon fluorescence microscopy," Biomed. Opt. Express **3**(9), 1972–1977 (2012).
21. S. Kivisto, T. Hakulinen, M. Guina, and O. G. Okhotnikov, "Tunable Raman soliton source using mode-locked Tm–Ho fiber laser," IEEE Photonics Technol. Lett. **19**(12), 934–936 (2007).
22. M. C. Chan, S. H. Chia, T. M. Liu, T. H. Tsai, M. C. Ho, A. A. Ivanov, A. M. Zheltikov, J. Y. Liu, H. L. Liu, and C.-K. Sun, "1.2-2.2 μm Tunable Raman Soliton Source Based on a Cr:Forsterite-Laser and a Photonic-Crystal Fiber," IEEE Photonics Technol. Lett. **20**(9–12), 920–922 (2008).
23. G. Chang, L.-J. Chen, and F. X. Kärtner, "Highly efficient Cherenkov radiation in photonic crystal fibers for broadband visible wavelength generation," Opt. Lett. **35**(14), 2361–2363 (2010).
24. F. M. Mitschke and L. F. Mollenauer, "Discovery of the soliton self-frequency shift," Opt. Lett. **11**(10), 659–661 (1986).
25. G. P. Agrawal, *Nonlinear Fiber Optics* (Academic Press, San Diego, 2007).
26. R. Yang, Y. Zheng, M. Burrows, S. Liu, Z. Wei, A. Nace, W. Guo, S. Kumar, G. Cotsarelis, and X. Xu, "Generation of folliculogenic human epithelial stem cells from induced pluripotent stem cells," Nat. Commun. **5**, 3071 (2014).
27. K. C. Sohn, G. Shi, S. Jang, D. K. Choi, Y. Lee, T. J. Yoon, H. Park, C. Hwang, H. J. Kim, Y. J. Seo, J. H. Lee, J. K. Park, and C. D. Kim, "Pitx2, a β-catenin-regulated transcription factor, regulates the differentiation of outer root sheath cells cultured in vitro," J. Dermatol. Sci. **54**(1), 6–11 (2009).
28. S. P. Tai, M. C. Chan, T. H. Tsai, S. H. Guol, L. J. Chen, and C.-K. Sun, "Two-photon fluorescence microscope with a hollow-core photonic crystal fiber," Opt. Express **12**(25), 6122–6128 (2004).
29. https://www.thermofisher.com/tw/zt/home/life-science/cell-analysis/labeling-chemistry/fluorescence-spectraviewer.html
30. R. M. Williams, W. R. Zipfel, and W. W. Webb, "Interpreting second-harmonic generation images of collagen I fibrils," Biophys. J. **88**(2), 1377–1386 (2005).

1. Introduction

Since its first demonstration in 1991 [1], two-photon fluorescence microscopy (TPFM), which utilizes two NIR photons to excite fluorescent molecules, has become an indispensable imaging tool due to its intrinsic optical sectioning capabilities and cellular to sub-cellular ultrahigh resolutions in three dimensions. TPFM is compatible with the current fluorescence microscopes and various biological fluorescence indicators, such as fluorescence proteins, quantum dots, nano-particles or even the auto-fluorescence of biological specimens [2, 3]. Moreover, since the working wavelength of most TPFM is located in the 0.7~1.35 μm bio-penetration window, TPFM offers the advantages of deeper penetration and much reduced photo-damage and photo-bleaching effects [4–9] over traditional one-photon fluorescence microscopy.

By one-photon fluorescence microscopes, biologists often utilize multiple fluorescence indicators with distinct absorption and emission spectra to label multiple targets within the same specimens. In the applications of multi-color one-photon fluorescence microscopy, observations of various organelles [10], different molecules [11], molecular co-localization

Biomedical Optics EXPRESS

[12, 13], and even molecular interactions [13] within single cells were achieved in earlierreports. In addition, it was also applied to investigate the mapping of distinct neural circuits in tissues [14] and the tracking of multiple cell populations such as in the studies of stem cell colonies [15], immune cell types [16], cancer cell growth and metastasis [17]. Though simultaneous multi-color one-photon fluorescence imaging is popular, few groups [18–20] reported multi-color TPFM of multiple fluorescence targets due to lack of simple multi-color femtosecond source which output wavelengths were closely matched to the 0.7-1.35 μm two-photon excitation spectrum of most fluorescence indicators.

In 2011, an excellent work demonstrated for multi-color TPFM and its applications on tracing the behaviors of cancer cells [18]. In that experiment, three bulky femtosecond lasers, including two Ti:Sapphire lasers (Tsunami & Mai-Tai, Spectral Physics) and one optical parametric oscillator OPO, were used simultaneously to excite four fluorescence indicators. In 2012, Mahou et al. reported another impressive work on three-color two-photon tissue imaging with a Ti:Sapphire laser and an OPO [19]. The three-color fluorescent indicators with different absorption spectra in a fly embryos were separately two-photon excited with the femtosecond pulses which were from a Ti:Sapphire laser, an OPO, and a wavelength mixing that of the two. These two excellent works, published in Nature Protocol [18] and Nature methods [19] separately, have a room for further improving the configuration of the multi-color TPFM. Furthermore, the high power femtosecond Ti:Sapphire lasers and OPOs were too bulky and expensive. For forming the multi-color source, several dichroic beam splitters, mirrors, or even high resolution delay lines, were required to spatially or even temporally combine multi-wavelength femtosecond pulses in order to form the common-path output to be delivered to the TPFM imaging system.

In 2012, Cornell's group have reported a simpler three-color TPFM based on an energetic laser and fiber-optic wavelength convertor [20]. In this work, an energetic 1.55-μm fiber laser with a μJ level output pulse energy was frequency-red-shifted to 1728 nm and 1900 nm by a large mode photonic crystal fiber (PCF). Next, the two wavelength red-shifted pulses and the residual 1550-nm pulses were separately frequency-doubled to 775, 864, and 950 nm by several BiBO nonlinear crystals. This good work also has a room for improvement in the wavelength conversion pathway and related system configuration. The two-step frequency conversion mechanism, including red-shift of wavelength by PCF and then frequency doubling by nonlinear crystals, was not quite efficient. Moreover, in the first step of frequency conversion mechanism inside nonlinear fibers, the minimum output wavelength was equal to the 1.55-μm pump wavelength and the maximum converted output wavelength was located around 2.2~2.3 μm, which is limited by the rapidly increased absorption of Silica fibers [21, 22]. With this approach, after frequency-doubling by nonlinear crystals, the wavelength range of multi-wavelength source is limited from 0.78-μm to 1.15-μm wavelength regime. Some ultra-violet or new IR fluorescent dyes within the entire 0.7~1.35 μm bio-penetration window cannot be two-photon pumped by this light source. Finally, many optical elements, including mirrors, frequency-doubling crystals, dichroic beam splitters, and lens, were required for generating, combining, frequency-doubling the three color femtosecond sources [20]. Additional elements could also increase the complexity, size, instabilities, and the insertion loss of the light source and the overall TPFM systems.

In this paper, a much simpler approach to the multi-wavelength femtosecond source within the 0.7~1.35 μm bio-penetration window and its application to multi-color TPFM were both reported. The new multi-wavelength femtosecond source consisted of a single 1.03-μm laser for pump and a nonlinear fiber for multiple wavelength conversion. Inside the nonlinear fiber, the 1.03-μm laser pulses were simultaneously blue-shifted to 0.6~0.8 μm and red-shifted to 1.2~1.4 μm region by the Cherenkov radiation [23] and fiber Raman gain [24, 25] effects. The two wavelength-converted beam and residual non-converted 1.03-μm pulses were naturally propagated in a common path (the same nonlinear fiber) to form a fiber-output three-color femtosecond laser. Then the three-color TPFM images of mouse skin hair

Biomedical Optics EXPRESS

follicles, which were simultaneously labeled by blue, green, and red fluorescent indicators in the different features of the same location, were performed by the demonstrated simple three-color femtosecond source. In this work, with the nonlinear fiber, a novel light source can work beyond the typical capabilities of a standard femtosecond solid-state laser. Such simplicity in wavelength conversion, wavelength tuning and overall TPFM microscopy yields the following advantages: efficient wavelength conversion in the nonlinear fiber less requirement for alignment and maintenance, and a compact and turn-key operation. As a consequence, the demonstrated ultra-simple multi-color TPFM, which mainly works within the 0.7~1.35 μm bio-penetration window, could be widely applicable as an excellent research tool for both fundamental biomedical research and future clinical applications.

2. Experimental setup and sample preparation

The inset of Fig. 1 shows the methods of this work. The 1.03-μm laser pulses were simultaneously blue-shifted to 0.6~0.8 μm and red-shifted to 1.2~1.4 μm region by a wavelength conversion fiber. Combining the converted 0.6~0.8 μm and 1.2~1.4 μm femtosecond radiations with the non-converted 1.03 μm pump pulses inside the same nonlinear fiber, a three-color femtosecond laser with a common-path output was demonstrated in the first part of this experiment. The generated blue-shifted to 0.6~0.8 μm Cherenkov radiation was utilized to pump the blue-indicators through the two-photon fluorescence process. The residual 1.03-μm pulses and Raman red-shifted 1.2~1.4 μm pulses were used to two-photon excite the green-indicators and red-indicators separately.

Figure 1 shows the schematics of the reported simple three-color femtosecond source and the related nonlinear microscope system. The three-color femtosecond light source was basically composed of a 1.03-μm air-cooled compact and portable Ytterbium femtosecond laser (Mikan, Amplitude Systems) and a single nonlinear PCF (SC-3.7-975, NKT Photonics). Typically, the Ytterbium laser emitted 250 fs pulses at a 1.03-μm central wavelength with a 1W average output power before the isolator and a 54.77 MHz repetition rate. An optical isolator was inserted between the 1.03-μm femtosecond laser and the fiber to prevent the backward reflection from the fiber facet which will destroy the femtosecond pulse generation of the 1.03-μm pump laser. The size of laser cavity was as small as 18 × 33 cm with a high portability and turn-key operation. The zero dispersion wavelength of the nonlinear PCF was 975 nm and the dispersion at 1.03 μm was around 13 ps/nm/km. The output end of the nonlinear fiber, playing a role as a delivery fiber and wavelength convertor, was directly connected to the input end of a home-made scanning system as shown in the remaining part of Fig. 1.

The home-build multi-wavelength TPFM was composed of galvanometer x-y scanners (6215H, Cambridge, USA), two plane-convex lens with a 5-cm and 15-cm focal length respectively, a dichroic beam splitter (FF660-Di02-25x36, Semrock), and a focusing objectives (LMPlan100X IR, Olympus). The generated multi-wavelength TPF signals were separated by the dichroic beam splitter, band-pass filtered by the emission filter, and detected by the photomultiplier tubes (PMTs) (R928P, Hamamatsu, Japan). The image acquisitions were carried out using lab-written LabVIEW software and a multichannel I/O board (PCI-6115, National Instruments). The average power illuminated on the sample was about 120 mW. The frame rate was 1 Hz with a 500-pixels-by-500-pixels resolution. Accordingly, the corresponding pixel dwelling time was 4 μsec. 4-frame averaging was performed for image quality in this work. Therefore, it takes 4 seconds to acquire a single image. The source and emission filter sets, which were placed on a mechanical filter wheel, were manually changed so that the typical time required for acquiring all 3-color images was around 30 seconds.

In the experiment, the used blue, green, and red indicators were DAPI, Alexa-Fluor 488, and Alexa-Fluor 594, respectively. The dyes were purchased from Invitrogen. The DAPI stained on cell nuclei and the Alexa-Fluor 488 as well as the Alexa-Fluor 594 stained on cytokeratin 17 and Pan-cytokeratin respectively in cells through affinity antibodies. All three

Biomedical Optics EXPRESS

indicators were used simultaneously to study the histology of mouse skin hair follicles on slide sections.

In order to demonstrate the uniqueness of the simple approach to multi-color TPFM, we chose the mouse skin hair follicles for this study because hair follicle is a small organ and pan-cytokeratin as well as cytokeratin 17 protein express in adjacent area of the hair follicle. Alexa fluor 594 and Alexa fluor 488 encamps un-overlapped excitation and emission wavelengths and were conjugated to specific secondary antibodies respectively. Yet, their respective first antibodies from different animal origin could be obtained to perform the co-staining experiment in this study. The skin samples with hair follicles were harvested from mouse, with approval of the Institutional Animal Care and Use Committee at the National Cheng Kung University (IACUC Approval No 103329). The DAPI was therefore labeled to the nuclei of dermal and epidermal cells. The Alexa-Fluor 488 and Alexa-Fluor 594 were labeled to the inner and outer root sheath of mouse skin hair follicles, respectively. Cryo-sections of the skin samples were prepared, fixed with 4% paraformaldehyde and rinsed with TBST (Tris Buffered Saline with Tween 20). Subsequently, the samples were reacted with 10μg / mL of first antibody-mix at 1:100 dilution in TBST with pan-cytokeratin antibody and cytokeratin 17 antibody. Pan-cytokeratin antibody (AE13), a mouse monoclonal antibody obtained from Santa Cruz Biotechnology, Inc., marked hair follicle cortex [26]. Cytokeratin 17 antibody, a rabbit monoclonal antibody obtained from Abcam plc, detected endogenous levels of total cytokeratin 17 protein expressed by outer root sheath of hair follicles [27]. After incubation overnight at 4°C and rinsing for three times, the samples were further incubated with a secondary antibody-mix with Alexa fluor 594 and Alexa fluor 488 in dark. The Alexa fluor 594 conjugated on an anti-mouse antibody and Alexa fluor 488 conjugated on an anti-rabbit antibody were purchased from Life Technologies Corp. and were diluted 1:200 in TBST (5μg/mL) for binding to their first antibody counterparts respectively. DAPI (diamidino-2-phenylindole) is a blue fluorescent probe that can bind to the minor groove of double stranded DNA. It was purchased from Life Technologies Corp. and 10 μg / mL was used to stain cell nucleus. Finally, the peak absorption of the blue, green, and red indicators were at wavelength of 359 nm, 499 nm, and 590 nm. On the other hand, the peak emission wavelengths of the three fluorescent indicators were 461 nm, 520 nm, and 618 nm, respectively.

Biomedical Optics EXPRESS

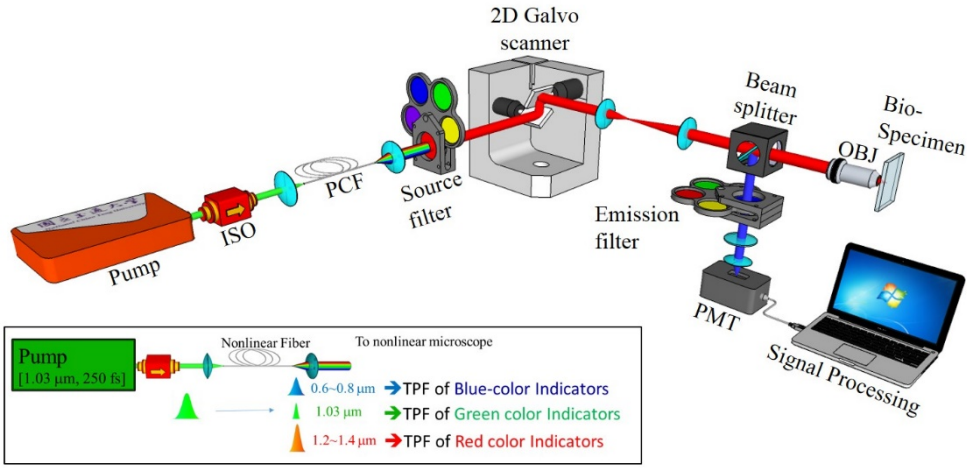

Fig. 1. Schematics and the working principle (shown in the inset) of the simple approach to multi-color two-photon fluorescence microscope. The three-color fiber-delivered femtosecond source was composed of a compact 1030 nm femtosecond laser as pump and a nonlinear fiber as a simultaneous wavelength up-and-down convertor. The fiber-output of the multi-color femtosecond source was then connected to the corresponding home-made nonlinear microscope to pump the blue, green, and red fluorescent indicators in the same specimen. For characterizing and avoiding the crosstalk between the R, G, and B channels, a source filter and a fluorescence filter were inserted after the source and before PMT separately. Pump: Compact 1.03-μm Ytterbium-doped femtosecond laser; ISO: optical isolator; PCF: photonic crystal fiber; OBJ: microscope objective; PMT; photomultiplier tube.

3. Experimental characterization of the three-color femtosecond sources

According to the earlier reports, with the same pulse energy, the two-photon excitation efficiency in TPFM is inversely proportional to the pulse width of the femtosecond source [28]. Therefore, the length of the wavelength conversion fiber, which is highly related with the output pulse width, should be carefully optimized. The fiber should be long enough to provide sufficient nonlinearity for wavelength conversion. On the other hand, the length of nonlinear fiber should be as short as possible to minimize dispersion induced pulse broadening. In this work, the optimized length of the nonlinear fiber was experimentally determined by measuring the output spectrum of the nonlinear PCFs with different lengths. Figure 2 shows power-dependent spectrum at the exit of nonlinear fiber with lengths of 100 cm, 14 cm, 7.5 cm, and 5 cm respectively. The broadband spectrum at fiber exit was measured by a single broadband spectrometer with a 500-1600 nm range (WaveScan USB VIS/IR, APE Berlin). As shown in Fig. 2(a), the power-dependent output spectra of a 100-cm nonlinear fiber shows that the threshold launched power for wavelength conversion was 100 mW. By adjusting the coupling power into the fiber, the central wavelength of blue-shifted and red-shifted emissions can also be also tuned. Similar power-dependent output spectra, shown in Fig. 2(b), were also observed with a 14-cm fiber. By changing the nonlinear phase-matching conditions inside the PCF, the central wavelength of blue-shifted and red-shifted emissions can also be adjusted. For the femtosecond sources operated within the 850 nm to 1100 nm window, in this experiment, only the green fluorescence indicators (Alexa-Fluor 488) can be efficiently two-photon excited. In the 14 cm nonlinear fiber, the threshold launched power was 250 mW for carrying out wavelength conversion outside of the 850 nm to 1100 nm wavelength window and pumping DAPI, Alexa-Fluor 488, and Alexa-Fluor 594 simultaneously. As indicated in Fig. 2(a) and 2(b), similar wavelength tuning range between 100-cm and 14-cm PCF shows that the generated blue and red shifted femtosecond pulses

Biomedical Optics EXPRESS

mainly experienced pulse-broadening effect in the last 86 cm of the fiber (i.e., 14 cm to 100 cm) and the fiber nonlinearity played a minor role.

Also evidenced from the experimental results of Fig. 2(a) and 2(b), we should continue cutting the nonlinear PCF in order to eliminate the pulse broadening effect. The power-dependent output spectra of other two fiber lengths, 5 cm and 7.5 cm were then measured and shown in Fig. 2(c) and 2(d), respectively. Figure 2(c) shows power-dependent spectra of nonlinear PCFs with length of 7.5 cm. With a 250-mW pump power inside the nonlinear fiber, the blue- and red-shifted components in the output spectrum were clearly observed. As the power increases from 250mW to 600mW, the central wavelength of blue-shifted and red-shifted emission can be tuned down from 0.86 to 0.70 μm and tuned up from 1.23 to 1.31 μm respectively. Figure 2(d) shows that no blue-shift and red-shift radiations were observed at the output of fiber even with a 500 mW coupling power inside the nonlinear fiber as the fiber length continues to be shortened to 5 cm.

On performance of nonlinear wavelength conversion for bio-medical applications, Fig. 2(a) to 2(d) show that the fiber-length-dependent spectra of 7.5-, 14- and 100-cm fibers all are long enough to provide sufficient nonlinearity. Based on the theory of basic fiber-optics [25], the over-length fiber, not only introduces extra dispersion but also severe pulse broadening. The temporal pulse broadening will degrade the excitation efficiencies of nonlinear signals. Therefore, in this experiment, a 7.5-cm fiber was selected as the nonlinear wavelength convertor to simultaneously transform the wavelength toward the blue and red side and minimize the image degradation from the excessive fiber dispersion.

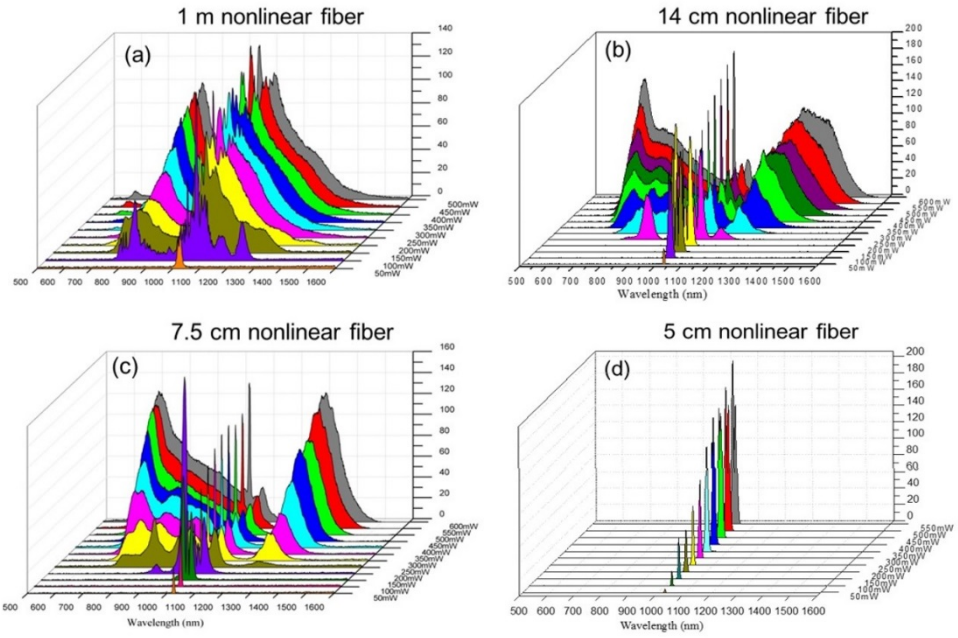

Fig. 2. The 3-D power-dependent output spectrum measurements at the end of the (a) 100 cm, (b) 14 cm, (c) 7.5 cm, and (d) 5 cm nonlinear fiber-optic wavelength convertor (FOWC). The values inserted in the figure represent the total average pump power after the nonlinear fiber.

Once the length of the nonlinear-wavelength-conversion fiber was determined, the coupling power into the fiber was determined next based on the peak absorption wavelength of the three fluorescent dyes. In this experiment, the coupling power into the nonlinear PCF was adjusted by simply rotating a neutral-density wheel. As mentioned earlier, the peak absorption wavelengths of the DAPI, Alexa-Fluor 488 and Alexa-Fluor 594 were 359, 499, and 590 nm, respectively. Figure 2(c) shows that the peak output wavelengths of the three-

Biomedical Optics EXPRESS

color femtosecond sources were 713, 1024, and 1302 nm respectively as the coupling increased to 550 mW in the 7.5-cm nonlinear fiber. The above peak output wavelengths mostly fit the theoretical two-photon absorption spectra of blue, green, and red fluorescent dyes. Therefore, as indicated by the red curve of Fig. 2(c), the output spectrum of the 7.5-cm nonlinear fiber with a 550 mW average power was used for the follow-up two-photon imaging experiments.

After determining the length of the nonlinear PCF and the launched power into the PCF, the next concern is how to avoid the crosstalks. For minimizing crosstalks between R, G, and B channels, the source filter sets were utilized between the nonlinear PCF and the nonlinear microscope, as shown in Fig. 1. First, the blue-shifted Cherenkov radiation was filtered out by a 945nm short-pass filter and a 750 nm colored-glass filter. In this experiment, a long-pass colored-glass filter with a more than 40-dB attenuation for photons of wavelength below 700 nm was used due to the fact that these photons will add a strong background on the two-photon fluorescence signals of the Red fluorescence indicators. On the other hand, for two-photon excited Green and Red fluorescence indicators, a bandpass filter and a 1060-nm long pass filter were separately utilized to filter out the residual pump and Raman-induced red-shifted components.

Figure 3 shows the filtered spectrum after the source filter and the corresponding time traces were measured by a background-free auto-correlator. Due to excess chirp from the fiber dispersion and nonlinearity, the pump pulses for the blue, green, and red fluorescent indicators were not transform-limited. The excitation pulses could be further compressed down by prism pair, grating pair or other bulky dispersive optical elements. In this work, for the simple overall system configuration, no compression units were adopted after the fiber. The two-photon fluorescent images, to be demonstrated later in Fig. 4 and Fig. 6, indicate that the un-compressed pulse widths were short enough for multi-color imaging.

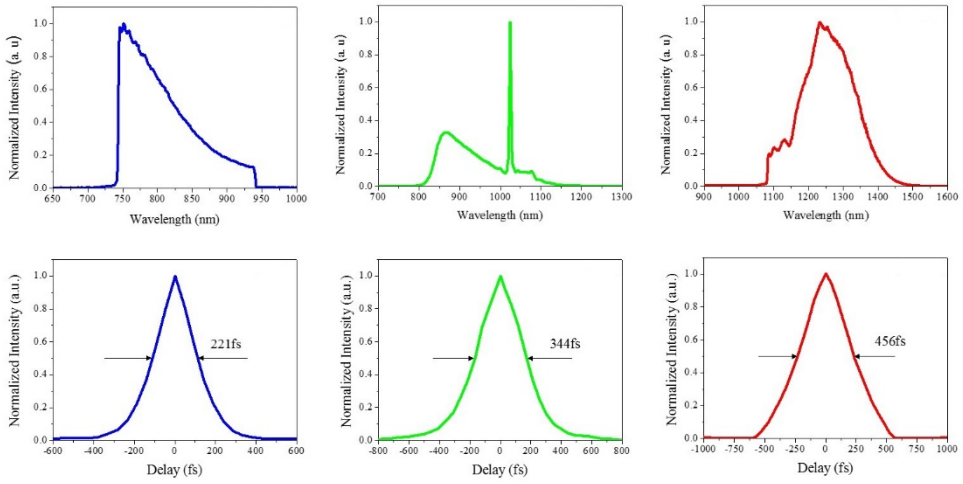

Fig. 3. The excitation spectra for pumping blue (a), green (b), and red (c) fluorescence indicators. The corresponding second harmonic background-free auto-correlation traces for them are shown in (d), (e), and (f), respectively

4. Minimization of channel crosstalk and demonstration toward simple three color TPFM

With the above fiber-output three-color femtosecond laser source, a series of experiments with different excitation and emission conditions were performed for evaluating the cross-talks between each of the channels. First, the tissues were labeled with one fluorescent indicators only and excited by one-color (blue-shifted 0.6~0.8 μm, residual 1.0 μm, or red-

Biomedical Optics EXPRESS

shifted 1.2~1.4 μm) by the source filters at a time. In the detection end, a series of band pass filters with different central wavelengths (447, 510, 520, 540, 562, 641 nm) and bandwidths (60, 84, 70, 50, 40, 75 nm) were placed before the PMT, as shown in Fig. 1, to examine the image quality and crosstalk in all channels.

Figure 4 shows the matrix images under different excitation and detection conditions when the dermal and epidermal cell of mouse skin hair follicles were stained by DAPI only. By changing the source filters, we excite the DAPI by one color (blue-shifted 0.6~0.8 μm, residual 1.0 μm, or red-shifted 1.2~1.4 μm) sequentially. And by changing the emission filters before PMT, the detection wavelength for imaging was also adjusted sequentially. The matrix images, as shown in Fig. 4(a), were formed by different excitation (each column) from various source filters and by different detection (each row) from various fluorescence filters. From the series matrix images with proper excitation and emission filters, we observed that neither residual 1.0 μm nor red-shifted 1.2~1.4 μm can pump the DAPI through the two-photon absorption process. The images with maximum contrast was acquired by the 510-nm filters. And the TPF images were also successfully performed with the 447- nm and 520-nm band-pass filters with acceptable contrast. Thus, the source filter was determined by the TPF matrix images of the green and red fluorescent dyes in the following experiments.

Similar matrix images of green fluorescent indicators (Alexa-Fluor 488), labeled to the inner root sheath of mouse skin hair follicles, were performed with different excitation conditions and emission filters. Based on the first and third columns in the matrix images, shown in Fig. 4(b), we can conclude the Alexa-Fluor 488 can be only two-photon excited by the residual 1.0 μm residual radiations. The maximum contrast images were acquired by the 520-nm filters, which consist of the peak emission wavelength of Alexa Fluor 488. The TPF images were also successfully performed with the 510 nm and 540 nm band-pass filters with similar contrast.

Finally, as shown in Fig. 4(c), the matrix images of red fluorescent indicators (Alex-Fluor 594), labeled to the outer root sheath of mouse skin hair follicles, were performed with different excitation conditions and emission filters. From Fig. 4(c), the TPF image of maximum contrast was acquired by the 1.2-1.3 μm red-shifted radiations and the 641-nm bandpass filter, which was shown in the bottom right image in Fig. 4(c). From the other sub-image in the matrix image, the Alexa-Fluor 594 can also be slightly pumped with the residual 1.0 μm radiations and some other bandpass filters. Fortunately, the excitation and emission conditions in those figures were very inefficient indicating the crosstalk will not be very serious.

Figure 4 (a) and 4(b) show that there were crosstalks between the TPF signals of the DAPI and Alexa-Fluor 488. Thus, 447 nm and 540 nm bandpass filters were selected for filtering out the fluorescence for DAPI and Alexa-Fluor 488 separately. Finally, in the matrix images shown in Fig. 4(c), the 641-nm bandpass filters were used for the Alexa-Fluor 594 TPF signals for maximum contrast.

Biomedical Optics EXPRESS

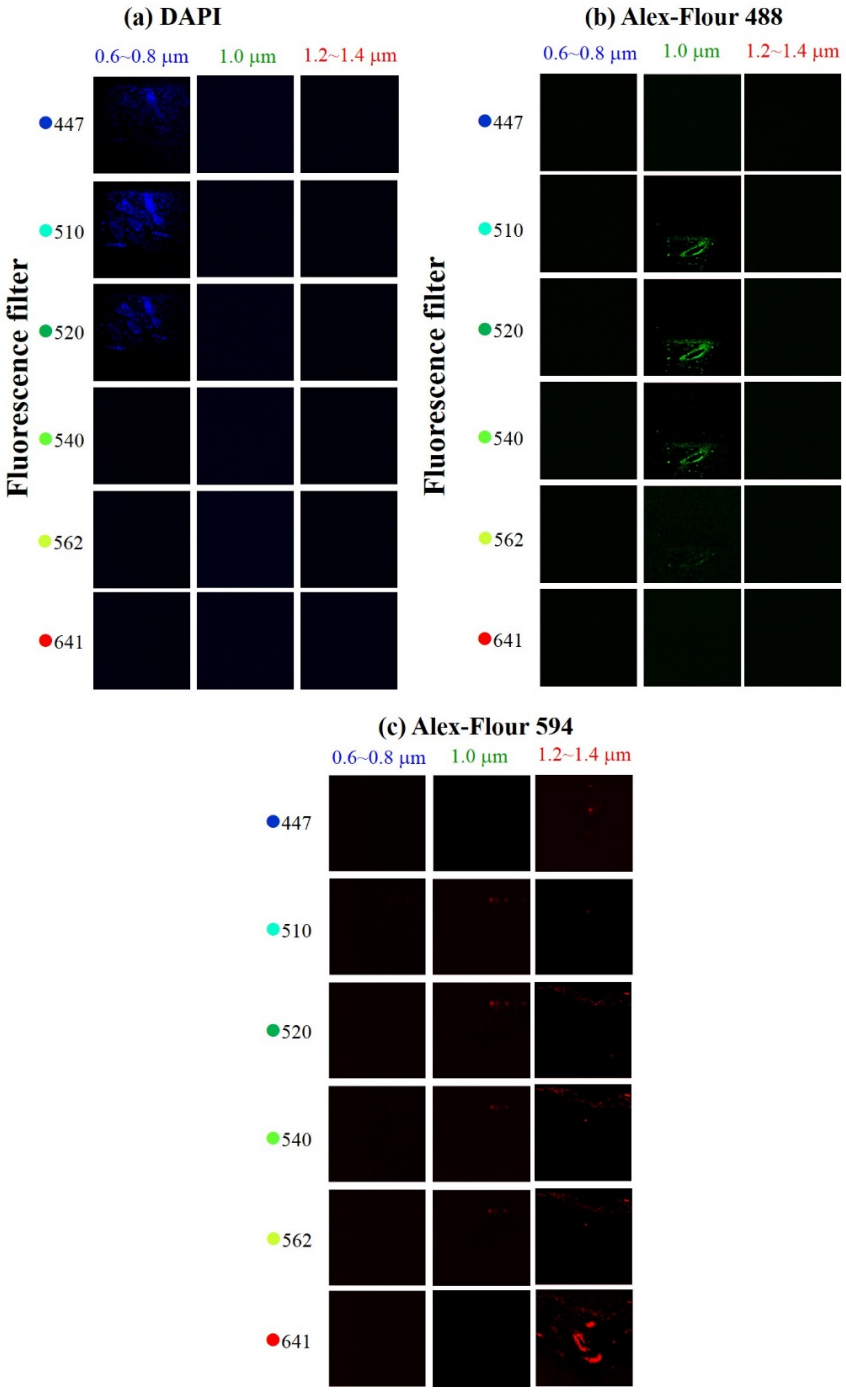

Fig. 4. Matrix two-photon fluorescence images of (a) **DAPI** fluorescent indicators, (b) **Alexa-Fluor 488** fluorescent indicators, and (c) **Alexa-Fluor 594** fluorescent indicators excited separately at blue-shifted 0.6~0.8 μm components (first columns), residual 1.030 μm (second columns), and 1.2~1.4 μm red-shifted components (third columns). Six bandpass filters of 447, 510, 520, 540, 562, and 641 nm (in each row) central wavelength were sequentially placed before the PMT. The matrix images were acquired for checking the crosstalks between the R, G, and B channel. The sizes of all the images were 310 μm by 310 μm.

Biomedical Optics EXPRESS

5. Simple RGB two-photon fluorescence microscopy

From a series of TPFM experiments with one labeled fluorescent indicator under different excitation and detection conditions, the parameters for performing three-color TPFM, including the length of the wavelength conversion PCF, the launched power into the fiber, and the cross-talk minimization, were determined. Before performing the multi-color TPFM, the spectra for pumping, excitation, and filtering were summarized based on the experimental results of matrix images shown in Fig. 4(a) to Fig. 4 (c). Figure 5 shows the emission spectra (solid lines) and two-photon pumping spectra (dashed lines) and the three-color fluorescent indicators [29]. And the inset of Fig. 5 shows the spectrum coverage of emission filters and source filters utilized for two-photon pumping.

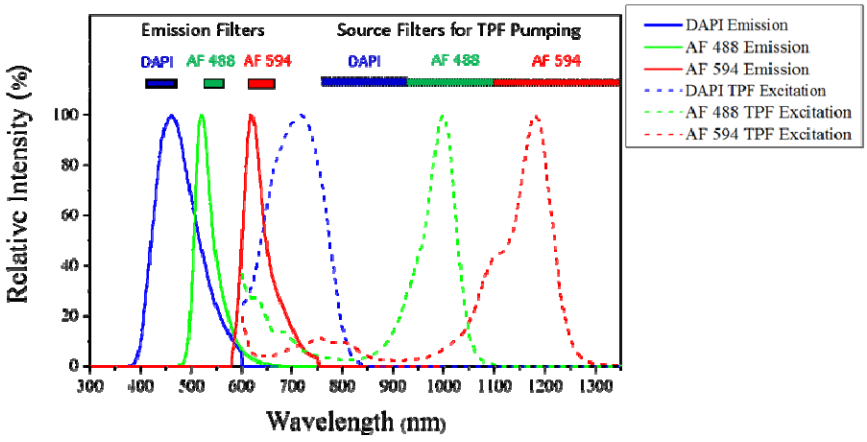

Fig. 5. The emission spectra (solid lines) and two-photon pumping spectra (dashed lines) of DAPI (Blue), Alexa-Fluor 488 (AF 488, Green), and Alexa-Fluor 594(AF 594, Red). The inset shows the spectrum coverage of emission filters before PMT and source filters after nonlinear fiber for two-photon pumping.

Finally, to demonstrate the feasibility of the novel three-color femtosecond fiber-optic source on multi-wavelength TPFM, the R, G, and B fluorescent indicators were labeled simultaneously to the tissues of mouse skin hair follicles. Figure 6 shows the three-color TPF imaging at the different spaces (each row). The signals from DAPI (blue, shown in Fig. 6(a) and 7(e)), Alexa Fluor 488 (green, shown in Fig. 6(b) and 6(f)), and Alexa Fluor 594 (red, shown in Fig. 6(c) and 6(g)) can thus be combined by computer post processing to obtain the hue of mouse skin hair follicles [Fig. 6(d) and 6(h)]. In all TPFM images, the sizes of all the images were 310 μm by 310 μm.

Biomedical Optics EXPRESS

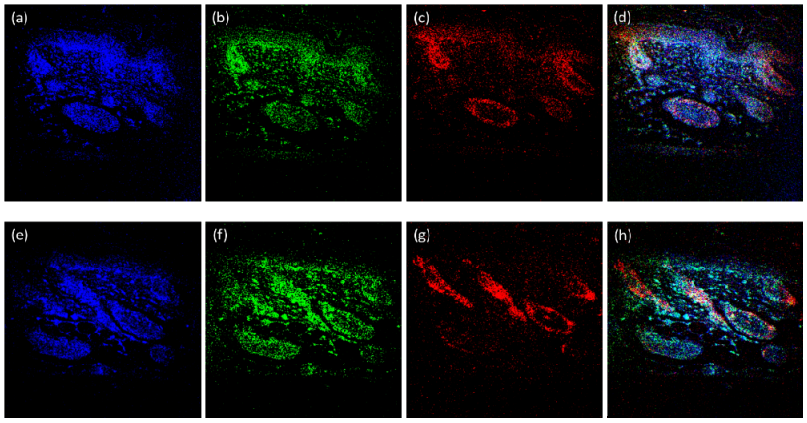

Fig. 6. Multi-color TPFM images of tissues at two different locations ((a)~(d) and (e)~(h)) in the mouse skin hair follicles performed by the simple microscope. Signals from DAPI (blue, Fig. 6(a) or 6(e)), Alexa Fluor 488 (green, Fig. 6(b) or 6(h)), and Alexa Fluor 594 (red, Fig. 6 (c) or 6(g)) channels were combined into rainbow images shown in Fig. 6(d) and 6(h). Image size: 310 μm by 310 μm.

In this work, we propose a novel and simple approach to multi-color TPFM on the mouse skin hair follicles by a 1.03-μm compact femtosecond laser and a simple nonlinear fiber. The output spectrum of the light source covers most of the 0.7~1.35 μm commercial biological fluorescent dyes. A systematic way to set up the microscope, including the fiber length selection from the output spectrum, the launched power determination based on the two-photon pumping spectra of each of the fluorescent indicators, and the crosstalk minimization between each of the channels in the matrix images shown in Fig. 4, was shown in this work. The overall cost of such novel apparatus consisting of a three-wavelength laser, a wavelength-conversion fiber with delivery optics, and a home-made nonlinear microscope was as low as 110 K USD in the proposed scheme shown in Fig. 1. Moreover, such multi-wavelength laser system can easily be operated as a workhorse with nearly a turn-key operation. This represents a much lower cost than those reported earlier [18–20]. The experimental work presented in this paper suggests that in the future, when performing multi-color TPFM with different fluorescent indicators, such as quantum dots, nano-particles, or other labeling materials, researchers only need simply to replace the light source with that of different wavelengths, to replace nonlinear fiber with different dispersion, nonlinear properties and corresponding filters.

Figure 7(a) illustrates that simultaneous imaging of all 3 fluorophores or of even more fluorescence indicators can be achieved by simply integrating additional independent parallel dichroic beam splitters and band-pass filters in the proposed system here. The main limitation for more-color imaging is the spectral-overlap-induced crosstalks of the emission spectra from different fluorescence indicators. On the other hand, if necessary, femtosecond pulses with more wavelengths can be achieved by the parallel fiber-optic wavelength convertors with different dispersion and nonlinear characteristics which is shown in Fig. 7(b). The only drawback of the proposed configuration in this work is a degraded signal intensity caused by dispersion in the fiber. Although the non-transform limited pulses could be compressed by external compressors after the nonlinear fiber, the compressor would introduce other issues such as the insertion loss, the difficulty in system size, alignment, and the system cost.

This new design toward multi-color TPFM makes a standard femtosecond solid-state lasers to perform beyond its standard operation wavelengths. Moreover, other imaging capabilities, for example, interpreting second-harmonic generation images of collagen I fibrils [30] from second harmonic generation, could be performed by the multi-color nonlinear microscopes.

Biomedical Optics EXPRESS

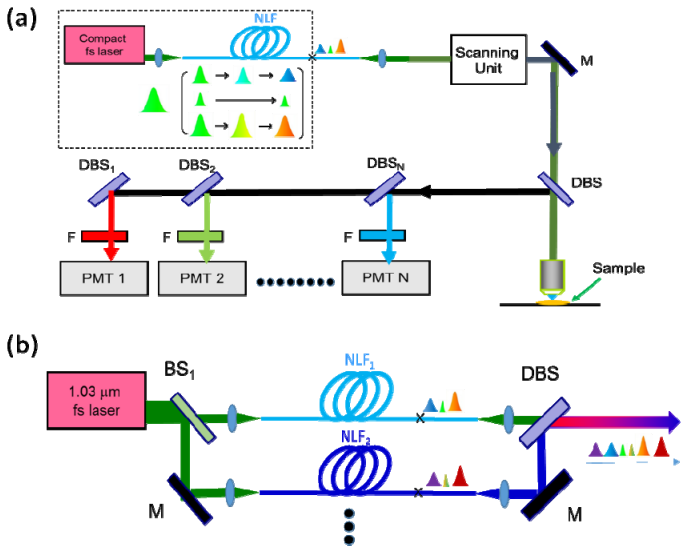

Fig. 7. Methods to (a) enable simultaneous imaging more fluorescence indicators by adding external parallel detection units; (b) generate more-wavelength femtosecond pulses by adding parallel nonlinear fibers. DBS: dichroic beam splitters; BS: beam splitters; M: Mirrors; NLF: nonlinear fiber and F: Filters.

6. Conclusions

In conclusion, we have reported a new approach to a simple multi-color TPFM based on an ultra-compact femtosecond laser and a simple nonlinear fiber. Inside the same nonlinear fiber, the 1.03 μm pump femtosecond pulses were simultaneously blue-shifted and red-shifted. Combining the wavelength-shifted 0.6~0.8 μm and 1.2~1.4 μm femtosecond radiations with a residual 1.03-μm pump, a fiber-delivered common-path three-color femtosecond laser were built up for exciting three different fluorescent indicators. The length of nonlinear fiber was experimentally optimized by measuring the output performance of the fiber. In the second part, the coupling power inside the nonlinear fiber was carefully selected to match the peak absorption spectrum of the R, G, and B fluorescent indicators. Finally, the real application on multi-color TPFM within the same specimen was experimentally demonstrated with the simple common-path three-color wavelength tunable femtosecond sources. The demonstrated ultra-simple multi-color TPFM can be widely applicable as an excellent research tool for both fundamental biomedical research and future clinical applications due to merits including a simple source and overall TPFM design, an easy wavelength tuning, an efficient wavelength conversion in the nonlinear fiber, a less requirement for alignment and maintenance, and compactness and turn-key operation of the source.

Funding

This research was supported in part by the National Science Council of Taiwan, ROC (MOST 100-2221-E-009-092-MY3, MOST 104-2221-E-009-155-MY3, MOST 105-2119-M-006-017) and the Department of Medical Research, Chi Mei Medical Center, Tainan 71004, Taiwan.

Acknowledgments

The authors acknowledge Prof. Tzu-Ming Liu of National Taiwan University for discussing some ideas. The authors also acknowledge the scientific discussions with Prof. Chi-Kuang Sun of National Taiwan University.